

Structure, Bonding, and Dynamics of Several Palladium η^3 -Allyl Carbene Complexes

Serena Filipuzzi, Paul S. Pregosin,* Alberto Albinati,* and Silvia Rizzato

Laboratory of Inorganic Chemistry, ETH HCI, Hönggerberg CH-8093 Zürich, Switzerland, and
Department of Structural Chemistry (DCSSI), University of Milan, 20133 Milan, Italy

Received October 22, 2007

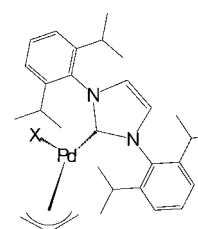
A series of Pd-allyl carbene complexes, $[\text{PdX}(\eta^3\text{-C}_3\text{H}_5)(\text{IPr})]$, **1** ($\text{X} = \text{a, Cl}^-, \text{b, Br}^-, \text{c, I}^-, \text{d, N}_3^-, \text{e, NCO}^-, \text{f, SCN}^-, \text{g, CN}^-, \text{h, OAc}^-, \text{i, OTf}^-, \text{j, 4-Me-pyridine}$), have been studied by one- and two-dimensional NMR techniques. ^{13}C , ^1H , and phase-sensitive NOE NMR studies on these relatively simple complexes reveal that (a) the *trans* influence of the carbene carbon in **1** seems to be smaller than that found for PPh_3 and other P-donor ligands, (b) the selective $\eta^3\text{-}\eta^1$ opening of the allyl is under electronic control, and (c) the rates of $\eta^3\text{-}\eta^1$ allyl isomerization depend on the X ligand. The solid-state structure of **1c** is reported, as well as selected ^{15}N chemical shift data for the coordinated carbene ligand.

Introduction

Carbene complexes have become increasingly important as ligands for transition metal catalyzed reactions.¹ Interestingly, in connection with palladium chemistry, they have begun to supplement the many known phosphine-supported C–C bond making catalysts.^{2–4} This has led to the synthesis and characterization of a number of new Pd-complexes containing N-heterocyclic carbene ligands.⁵ Although N-heterocyclic carbene ligands are generally thought to be good σ -donors,⁶ there are relatively few solution studies on their complexes of palladium(II) that address this subject. In contrast to the modest number of solution (and specifically NMR) results, one finds an increasing number of solid-state Pd-carbene structures in the literature.^{3,7–9}

The dynamics of palladium allyl complexes have been under investigation for more than 30 years.¹⁰ It is generally accepted^{10–15} that an η^3 to η^1 mechanism can operate, although this cannot

always be unequivocally proven. It has been suggested¹⁵ that this allyl isomerization can involve a dissociative mechanism, and in some cases there is evidence to support this assumption.¹³ Further, it is now well-known that allyl isomerization in Pd-complexes can be markedly affected by the nature of the other ligands;¹¹ that is, the allyl isomerization from an η^3 to an η^1 species can be under either steric or electronic control.¹¹



1 X = a, Cl, b, Br, c, I, d, N₃, e, NCO, f, SCN, g, CN, h, OAc, i, OTf, j, 4-Me-pyridine

We report here ^1H , ^{13}C , and NOE NMR studies on the relatively simple Pd N-heterocyclic carbene allyl complexes

(1) (a) Arndt, S.; Schrock, R. R.; Mueller, P. *Organometallics* **2007**, *26* (5), 1279–1290. (b) Schrock, R. R. *Adv. Synth. Catal.* **2007**, *349* (1+2), 25. (c) Schrock, R. R. *Adv. Synth. Catal.* **2007**, *349* (1+2), 41–53. (d) Schrock, R. R.; Czekelius, C. *Adv. Synth. Catal.* **2007**, *349* (1+2), 55–77. (e) Grubbs, R. H. *Adv. Synth. Catal.* **2007**, *349* (1+2), 23–24. (f) Grubbs, R. H. *Adv. Synth. Catal.* **2007**, *349* (1+2), 34–40. (g) Mohapatra, D. K.; Ramesh, D. K.; Giardello, M. A.; Chorghade, M. S.; Gurjar, M. K.; Grubbs, R. H. *Tetrahedron Lett.* **2007**, *48* (14), 2621–2625. (h) Berlin, J. M.; Campbell, K.; Ritter, T.; Funk, T. W.; Chlenov, A.; Grubbs, R. H. *Org. Lett.* **2007**, *9* (7), 1339–1342.

(2) Douthwaite, R. E. *Coord. Chem. Rev.* **2007**, *251* (5+6), 702–717.

(3) Viciu, M. S.; Zinn, F. K.; Stevens, E. D.; Nolan, S. P. *Organometallics* **2003**, *22* (16), 3175–3177.

(4) Viciu, M. S.; Germaneau, R. F.; Navarro-Fernandez, O.; Stevens, E. D.; Nolan, S. P. *Organometallics* **2002**, *21* (25), 5470–5472.

(5) (a) Grundemann, S.; Albrecht, M.; Kovacevic, A.; Faller, J. W.; Crabtree, R. H. *J. Chem. Soc., Dalton Trans.* **2002**, (10), 2163–2167. (b) Loch, J. A.; Albrecht, M.; Peris, E.; Mata, J.; Faller, J. W.; Crabtree, R. H. *Organometallics* **2002**, *21* (4), 700–706. (c) Ketz, B. E.; Cole, A. P.; Waymouth, R. M. *Organometallics* **2004**, *23* (12), 2835–2837. (d) Bertogg, A.; Camponovo, F.; Togni, A. *Eur. J. Inorg. Chem.* **2005**, (2), 347–356. (e) Navarro, O.; Marion, N.; Mei, J.; Nolan, S. P. *Chem. Eur. J.* **2006**, *12* (19), 5142–5148. (f) Amblard, F.; Nolan, S. P.; Schinazi, R. F.; Agrofoglio, L. A. *Tetrahedron* **2005**, *61* (3), 537–544. (g) Singh, R.; Viciu, M. S.; Kramareva, N.; Navarro, O.; Nolan, S. P. *Org. Lett.* **2005**, *7* (9), 1829–1832.

(6) (a) Diez-Gonzalez, S.; Nolan, S. P. *Coord. Chem. Rev.* **2007**, *251* (5–6), 874–883. (b) Heckenroth, M.; Neels, A.; Stoekli-Evans, H.; Albrecht, M. *Inorg. Chim. Acta* **2006**, *359* (6), 1929–1938.

(7) Chernyshova, E. S.; Goddard, R.; Poerschke, K.-R. *Organometallics* **2007**, *26* (13), 3236–3251.

(8) Viciu, M. S.; Navarro, O.; Germaneau, R. F.; Kelly, R. A., III; Sommer, W.; Marion, N.; Stevens, E. D.; Cavallo, L.; Nolan, S. P. *Organometallics* **2004**, *23* (7), 1629–1635.

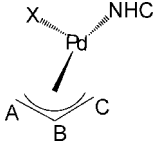
(9) (a) Fuerstner, A.; Seidel, G.; Kremzow, D.; Lehmann, C. W. *Organometallics* **2003**, *22* (5), 907–909. (b) Fuerstner, A.; Krause, H.; Lehmann, C. W. *Chem. Commun.* **2001**, (22), 2372–2373.

(10) Vrieze, K. In *Dynamic Nuclear Magnetic Resonance Spectroscopy*; Jackman, L. M., Cotton, F. A., Eds.; Academic Press: New York, 1975; p441–483.

(11) (a) Breutel, C.; Pregosin, P. S.; Salzmann, R.; Togni, A. *J. Am. Chem. Soc.* **1994**, *116* (9), 4067–4068. (b) Herrmann, J.; Pregosin, P. S.; Salzmann, R.; Albinati, A. *Organometallics* **1995**, *14* (7), 3311–3318. (c) Pregosin, P. S.; Salzmann, R. *Coord. Chem. Rev.* **1996**, *155*, 35–68. (d) Kumar, P. G. A.; Dotta, P.; Hermatschweiler, R.; Pregosin, P. S.; Albinati, A.; Rizzato, S. *Organometallics* **2005**, *24* (6), 1306–1314.

(12) (a) Ogasawara, M.; Takizawa, K.; Hayashi, T. *Organometallics* **2002**, *21* (22), 4853–4861. (b) Cesarotti, E.; Grassi, M.; Prati, L.; Demartin, F. *J. Organomet. Chem.* **1989**, *370*, 407–419. (c) Steinhagen, H.; Reggelin, M.; Helmchen, G. *Angew. Chem., Int. Ed. Engl.* **1997**, *36* (19), 2108–2110. (d) Sprinz, J.; Kiefer, M.; Helmchen, G.; Reggelin, M.; Huttner, G.; Zsolnai, L. *Tetrahedron Lett.* **1994**, *35*, 1523–1526. (e) Crociani, B.; Antonaroli, S.; Bandoli, G.; Canovese, L.; Visentin, F.; Uguagliati, P. *Organometallics* **1999**, *18* (7), 1137–1147. (f) Faller, J. W.; Wilt, J. C. *Organometallics* **2005**, *24* (21), 5076–5083. (g) Faller, J. W.; Sarantopoulos, N. *Organometallics* **2004**, *23* (9), 2008–2014.

(13) Gogoll, A.; Ornebro, J.; Grennberg, H.; Bäckvall, J. E. *J. Am. Chem. Soc.* **1994**, *116*, 3631.

Table 1. ^{13}C NMR Data for the Allyl Groups for Complexes **1a–j** (CD_2Cl_2 , 500 or 700 MHz)


complex	allyl carbon		
	A	B	C
Cl, 1a	71.4	114.1	49.8
Br, 1b	71.2	114.1	53.3
I, 1c	68.3	113.1	59.0
N_3 , 1d	71.6	116.3	48.1
NCO, 1e	70.1	114.8	47.5
SCN, 1f	76.7	116.7	56.2
CN, 1g	60.8	117.0	58.3
CH_3CO_2 (at 203 K), 1h	71.0	114.2	45.3
CF_3SO_3 (at 273 K), 1i	80.6	115.7	45.1
4-MePy, 1j	76.3	119.3	50.9

$[\text{PdX}(\eta^3\text{-C}_3\text{H}_5)(\text{IPr})]$, **1**, containing the carbene ligand [*N,N*-bis(2,6-diisopropylphenyl)imidazol-2-ylidene] (=IPr). We suggest that there are specific dynamics associated with the $\eta^3\text{-}\eta^1\text{-}\eta^3$ isomerization mechanism and that the *trans* influence of the bulky carbene in these Pd(II) complexes is strong, but not necessarily greater than a P-donor.

Results and Discussion

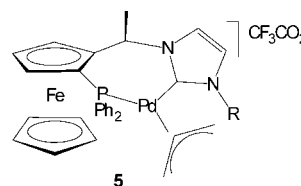
The complexes $[\text{PdX}(\eta^3\text{-C}_3\text{H}_5)(\text{IPr})]$, **1**, were prepared by substitution of the chloride ligand from the commercially available complex **1a**. For **1a–1g** it was sufficient to stir an excess of the appropriate anion with **1a** overnight; however for **1h** and **1i**, the chloride was abstracted with the appropriate silver salt, and for **1j**, the chloride abstraction was followed by addition of 4-picoline. A number of closely related Pd-allyl-carbene complexes are known.^{7,8,16}

The complexes were characterized via ^1H and ^{13}C NMR studies together with IR, mass spectral, and microanalytical data. Table 1 provides the ^{13}C data for the allyl ligand, and Table S1 (in the Supporting Information) provides an overview of all relevant ^1H and ^{13}C data for the complexes. We assign the SCN^- complex as having a Pd–S bond.¹⁷ The more labile complexes **1h** and **1i** require additional comment, and these will be made in the section on the dynamics.

^{13}C Chemical Shifts. The ^1H assignments for the η^3 -allyl group were made using intra- and interligand NOESY contacts, together with literature chemical shift data^{10–16} and the magnitudes of the various spin–spin coupling constants. These proton data were then used to assign the ^{13}C signals via correlation spectroscopy. Figure 1 shows a slice through the $^{13}\text{C}, ^1\text{H}$ HMQC

correlation¹⁸ for **1b**, in the high-frequency carbene ^{13}C region, as well as the conventional ^1H spectrum. There are five nonequivalent allyl protons signals, a singlet for the equivalent heterocyclic olefinic protons, an apparent A_2X spin system¹⁹ for the aromatic ring protons, plus two methine and four methyl resonances from the *i*-Pr groups. We will return to the numbers of observed *i*-Pr resonances in connection with the dynamics. From Figure 1 it is clear that one can use the three-bond interaction from the heterocyclic olefinic protons to locate the carbene carbon signals, all of which fall in the narrow range 182–186 ppm. Interestingly, there is also a strong three-bond interaction between the allyl *anti* proton *trans* to the carbene ligand and the carbene carbon. Given the unexpected relative similarity of these ^{13}C carbene chemical shifts, we have measured the natural abundance ^{15}N NMR spectra ($I = 1/2$, natural abundance = 0.36%) for three complexes, $\text{X} = \text{Cl}^-$, SCN^- , and CN^- as a check (see Figure 2). Indeed, all three ^{15}N resonances appear in the narrow range $\delta = -187$ to -189 (see Table 2), suggesting, together with the carbene ^{13}C data, that these carbene ligands are not markedly affected by the differing X ligands. For the selection of complexes in Table 2, the total ^{15}N chemical shift range is ca. 18 ppm.

The two terminal allyl ^{13}C chemical shifts reflect the difference in *trans* influence, with position A pseudo-*trans* to the carbene carbon appearing at much higher frequency. Specifically, for this allyl carbon, A, the values appear in the region ca. 61–81 ppm, whereas those for the allyl carbon C (pseudo-*trans* to the X ligand) fall in the range ca. 45–59 ppm. Within any one complex, the difference between the two terminal allyl ^{13}C chemical shifts, $\Delta\delta$, is largest for the triflate, 25.5 ppm, and smallest for the cyanide derivative, 2.5 ppm. It is informative to compare these ^{13}C data from Table 1 with those for the PPh_3 , **2**,²⁰ phosphoramidite, **3**,²¹ and P^tPr_3 , **4**,²² chloro-complexes (see Scheme 1). For **2**, these terminal allyl carbons appear at 62.0 ppm (*trans* to Cl) and 79.4 ppm (*trans* to P), for **3** at 50.8 ppm (*trans* to Cl) and 81.4 ppm (*trans* to P), and for **4** at 51.3 (*trans* to Cl) and 79.2 (*trans* to P) so that, based on these data, the *trans* influence of the carbene carbon in **1** seems to be *smaller* than that found for these P-donors. Visentin and Togni²³ have recently prepared several salts of structure **5** and found the two allyl termini to have similar ^{13}C chemical shifts, although for $\text{R} = t\text{-Bu}$, the allyl CH_2 *trans* to P appears at somewhat higher frequency. Further, their observed low enantioselectivities in allylic amination chemistry support the view that the carbene and phosphorus donors have similar *trans* influences.



Returning to the ^{13}C data for **1**, if one centers on allyl carbon C, *trans* to X, one sees that this chemical shift increases ca. 14 ppm across the series as a function of the donor strength of X,

(14) Kollmar, M.; Helmchen, G. *Organometallics* **2002**, 21 (22), 4771–4775.

(15) (a) Albinati, A.; Kunz, R. W.; Ammann, C. J.; Pregosin, P. S. *Organometallics* **1991**, 10 (6), 1800–1806. (b) Albinati, A.; Ammann, C.; Pregosin, P. S.; Ruegger, H. *Organometallics* **1990**, 9 (6), 1826–1833.

(16) Ding, Y.; Goddard, R.; Poerschke, K.-R. *Organometallics* **2005**, 24 (3), 439–445.

(17) The IR stretching vibration at 2104 cm^{-1} (see Burmeister, J. L. *Coord. Chem. Rev.* **1966**, 1, (1–2), 205–221), the trends observed for the allyl ^{13}C chemical shifts, and the absence of a ^{15}N signal in the N,H correlation are all consistent with this assignment. We do observe a second species in solution (ca. 3%) which is in exchange with the major component, and this might be the N-isomer. Burmeister assigns an S–C vibration at ca $780\text{--}960\text{ cm}^{-1}$ to the Pd–NCS isomer. This vibration is absent in our complex.

(18) von Philipsborn, W. $^{13}\text{C}, ^1\text{H}$ HMQC methods, in connection with inverse detection, can afford markedly better S/N—as much as a factor of 30!—relative to the conventional 1-D ^{13}C NMR spectrum. *Chem. Soc. Rev.* **1999**, 28, 95–105.

(19) For one complex, $\text{X} = \text{CN}$, it was possible to resolve these *meta*-aryl carbene nonequivalent protons at 700 MHz (see Figure 2).

(20) Shaw, B. L.; Mann, B. E.; Pietropaolo, R. *Chem. Commun.* **1971**, (15), 790–791.

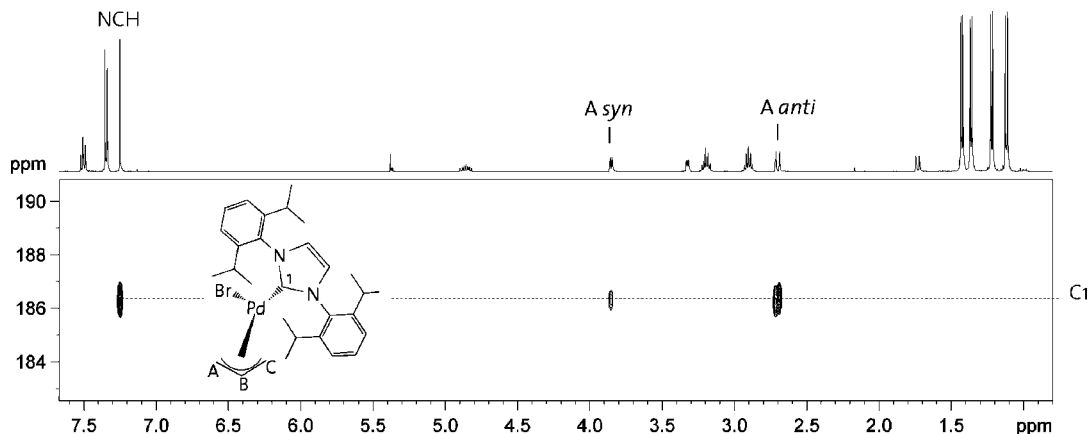


Figure 1. A slice through the ^{13}C , ^1H HMQC correlation for **1b**, in the high-frequency carbene ^{13}C region. The top trace shows the conventional ^1H spectrum (500 MHz, CD_2Cl_2).

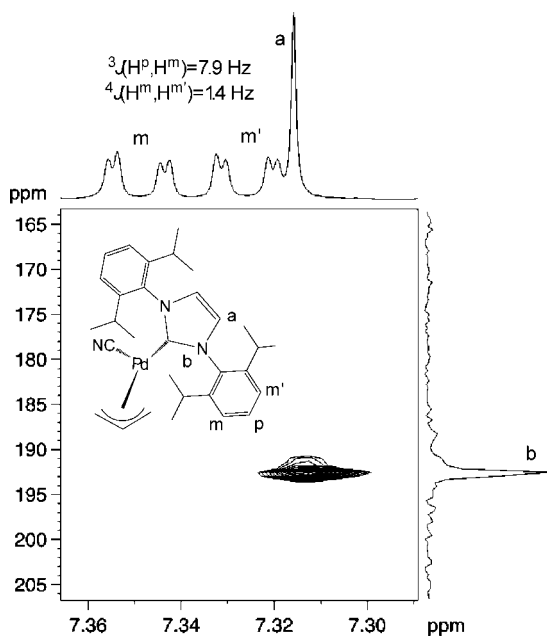


Figure 2. ^{15}N , ^1H HMQC correlation for the cyanide complex **1g**. Note that the correlation involves the two equivalent olefinic protons of the carbene and that the two *meta* protons of the aromatic ring are now resolved. The vertical axis shows a slice through the 2-D map (CD_2Cl_2 , 700 MHz).

with cyanide and iodide affording the largest values. The change in the chemical shift of the allyl carbon *trans* to the carbene atom, A, ca. 12 ppm across the series, is a little surprising and suggests that the effect of the *cis* ligand X (or a combination of steric and electronic effects) is significant. In a recent series of papers, Pörschke and co-workers^{7,16} have prepared a number of Pd-carbene allyl complexes. One of these, **6**, shows terminal allyl ^{13}C shifts of 49.3 ppm (*trans* to carbene) and 58.9 ppm (*trans* to methyl), suggesting, again, that for this type of complex the carbene ligand does not have the strongest *trans* influence and that the effect of the *cis* ligand can be quite marked.

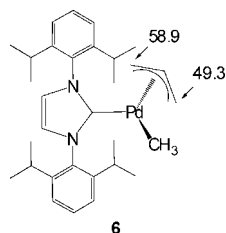
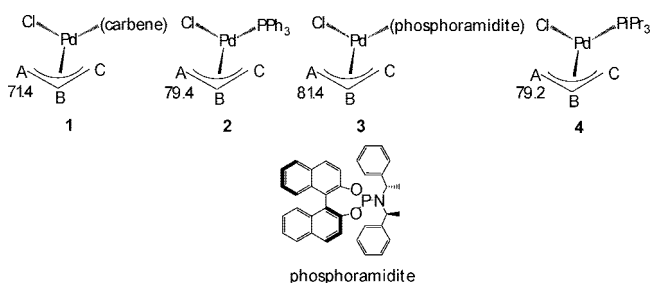


Table 2. ^{15}N NMR Data for the Imidazole Nitrogen in Selected Carbene Complexes for the Pd-Complexes, 700 MHz in CD_2Cl_2

compound	δ (ppm) ^a	δ (ppm) ^b	reference
[PdCl(C ₃ H ₅)(IPr)], 1a	-188.6	191.8	this work
[Pd(SCN)(C ₃ H ₅)(IPr)], 1f	-187.1	193.3	this work
[Pd(CN)(C ₃ H ₅)(IPr)], 1g	-187.9	192.5	this work
bis(carbene)mercury(II)	-193.7	186.7	^d
bis(carbene)copper(I)	-180.8	199.6	^e
bis(carbene)silver(I)	-179.1	201.3	^e
bis(carbene)nickel(0)	-193.2	187.2	^f
bis(carbene)platinum(0)	-189.2	191.2	^f
<i>N,N'</i> -bis[(<i>R</i>)-2-methylferrocen-1-yl]imidazol-2-ylidene ^c	-188.2	192.2	^g
1,3-dimethylimidazol-2-ylidene ^c	-197.3	183.1	^g

^a Referenced to CH_3NO_2 . ^b Referenced to liquid NH_3 . ^c As free carbene ligand. ^d Arduengo, A. J., III, Harlow, R. L., Marshall, W. J., Prakash, T. K. *Heteroat. Chem.* **1996**, 7 (6), 421–426. ^e Arduengo, A. J., III, Dias, H. V. R., Calabrese, J. C., Davidson, F. *Organometallics* **1993**, 12 (9), 3405–3409. ^f Arduengo, A. J., III, Gamper, S. F., Calabrese, J. C., Davidson, F. *J. Am. Chem. Soc.* **1994**, 116 (10), 4391–4394. ^g Bertogg, A., Camponovo, F., Togni, A. *Eur. J. Inorg. Chem.* **2005**, (2), 347–356.

Scheme 1



The source of this possible *cis* influence is not immediately obvious. In kinetic studies involving Pt(II) (where one discusses the “effect” and not the “influence”), van Eldik and co-workers²⁴ state that the *trans* effect of a metal–carbon bond on the rate of square-planar substitution reactions is very significant, but little is known about its *cis* effect. Further, they state that changing from a nitrogen σ -donor to a stronger carbon σ -donor in the *cis* position results in a *deceleration* of the substitution rate.

(21) Boele, M. D. K.; Kamer, P. C. J.; Lutz, M.; Spek, A. L.; de Vries, J. G.; van Leeuwen, P.; van Strijdonck, G. P. E. *Chem.–Eur. J.* **2004**, 10 (24), 6232–6246.

(22) Krause, J.; Goddard, R.; Mynott, R.; Poerschke, K.-R. *Organometallics* **2001**, 20 (10), 1992–1999.

(23) Visentin, F.; Togni, A. *Organometallics* **2007**, 26 (15), 3746–3754.

(24) (a) Jaganyi, D.; Reddy, D.; Gertenbach, J. A.; Hofmann, A.; van Eldik, R. *Dalton Trans.* **2004**, 2, 299–304. (b) Hofmann, A.; Dahlenburg, L.; van Eldik, R. *Inorg. Chem.* **2003**, 42 (20), 6528–6538.

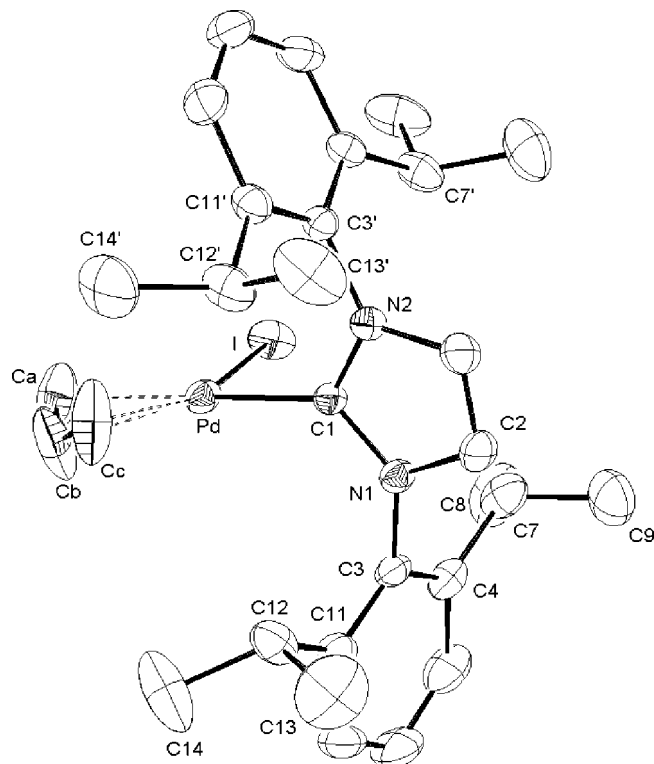


Figure 3. ORTEP view of **1c**. Thermal ellipsoids are drawn at 50% probability. Selected bond lengths (Å) and bond angles (deg): Pd–C(1), 2.040(2); Pd–Ca, 2.164(3); Pd–Cb, 2.110(4); Pd–Cc, 2.103(4); Pd–I, 2.6498(4); Ca–Cb, 1.303(6); Cb–Cc, 1.310(6); N(1)–C(1), 1.354(3); N(2)–C(1), 1.357(3); N(1)–C(2), 1.388(3); N(1)–C(3), 1.443(3); N(2)–C(1), 1.357(3); N(2)–C(15), 1.387(3); N(2)–C(3'), 1.444(3); C(1)–Pd–I, 101.33(7); Cc–Pd–I, 157.7(1); Cb–Pd–I, 125.5(1); Ca–Pd–I, 91.0(1); C(1)–Pd–Cc, 99.3(1); C(1)–Pd–Cb, 132.8(1); C(1)–Pd–Ca, 167.4(1); Cc–Pd–Ca, 68.2(2); Ca–Cb–Cc 132.5(5), I–Pd–C(1)–N(1), –89.4(2); I–Pd–C(1)–N(2) 94.7(2); C(1)–N(1)–C(3)–C(4), 96.7(3).

Continuing, Romeo and co-workers²⁵ reported a kinetic study involving cyclometalation, where the metal–carbon bond was located in the *cis* position and concluded that, again, the presence of a strong σ -donor carbon group decelerated the rate of ligand substitution. Consequently, there are indications from the literature that the *cis* and *trans* effects may be quite different, indeed work in opposite directions. This is in agreement with both our carbon data and the rate constants to be presented in the section on the dynamics.

X-ray Data. The solid-state structure of the iodo-complex, **1c**, was determined by X-ray diffraction methods, and a view of this compound along with selected bond lengths and bond angles is given in Figure 3.

The immediate coordination sphere about the Pd-atom consists of the three carbons of the η^3 -allyl group, the iodide, and C(1) of the carbene ligand. As expected, based on the recent literature,⁸ the Pd–C separation, 2.164(3) Å for the allyl carbon C(a), pseudo-*trans* to the carbene, is slightly longer than the Pd–C distance, Pd–C(c), 2.103(4) Å, pseudo-*trans* to the iodide. The Pd–C (carbene) separation, 2.040(2) Å, is in excellent agreement with the reported value⁸ for **1a**, 2.040(11) Å. The two C–N bond lengths, N(1)–C(1) Å, 1.354(3), and N(2)–C(1), 1.357(3) Å, in **1c** are not significantly different.

The bond angle C(1)–Pd–I, 101.33(7)°, suggests some steric repulsion between the carbene and iodide ligands. Further, the torsion angles I–Pd–C(1)–N(1), –89.4(2)°, and I–Pd–C(1)–N(2), 94.7(2)°, place the heterocyclic ring almost perpendicular to the

Table 3. Comparison of the Terminal Pd–Allyl Bond Lengths for **1a–1c** and Model Complexes

	Pd–C _A (Å)	Pd–C _C (Å)	reference
[PdI(C ₃ H ₅)(IPr)], 1c	2.164(3)	2.103(4)	this work
[PdBr(C ₃ H ₅)(IPr)], 1b	2.177(5)	2.094(7)	this work
[PdCl(C ₃ H ₅)(IPr)], 1a	2.201(17) ^a	2.110(16) ^a	8
[PdCl(C ₃ H ₅)(SIPr)]	2.211(6)	2.098(6)	4
[PdBr(C ₃ H ₅)(carbene)]	2.209(4)	2.123(4)	27

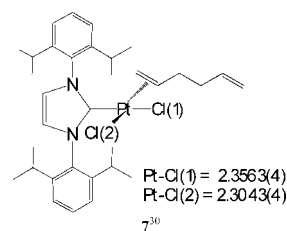
^a The experimental error is relatively large, but based on the two model complexes shown, the ca. 2.20 Å value is reasonable.

I–Pd–C(1) plane, and the angle C(1)–N(1)–C(3)–C(4), 96.7(3)°, confirms that the aromatic ring is about perpendicular to the carbene ring.

We have also determined the structure of the bromo complex **1b**.²⁶ Although disorder in the occluded solvent complicates the refinement, the various Pd–allyl separations are well defined. These distances, together with those for a number of related chloro analogues,^{4,8,27} are shown in Table 3.

Interestingly, the Pd–C_A separation (that which is *cis* to X) decreases such that Cl > Br > I. It seems that this allyl carbon is more strongly bound in the iodide than in the chloride. The table also shows two further reference carbene allyl chloro-complexes which possess very similar Pd–C_A distances.

Having raised the subject of relative *trans* influence in connection with the measured ¹³C data, we note that Sanford et al.²⁸ mention that the Ru–P distance barely changes upon substituting the *trans* ligand from PCy₃ to IMes. Specifically in their RuCl₂(CHPh)(PCy₃)₂ complex, the Ru–P distances are 2.4097(6) and 2.4221(6) Å, whereas the Ru–P distance in the RuCl₂(CHPh)(PCy₃)(IMes) analogue is 2.419(3) Å. Clearly, here, the crystallographic *trans* influences for the PCy₃ and IMes ligands are similar. Further, in a series of carbene complexes involving Pt(II), Nolan and co-workers^{29,30} find that the Pt–Cl separations are consistent with a strong but not extreme *trans* influence (see 7). For comparison, we note that Cárdenas et al. find a much longer Pt–Cl separation, 2.417(2) Å, in a cyclometalated complex of platinum(II).³¹



Dynamics. Figure 4 shows the exchange cross-peaks from the phase-sensitive NOESY spectrum for the bromo-complex **1b**. One can recognize a selective exchange process within the allyl protons (indicated by the dotted line) as well as some exchange associated with the two *i*-Pr resonances (solid lines), despite the seemingly sharp proton line widths. Analysis of the

(25) Romeo, R.; Plutino, M. R.; Scolaro, L. M.; Stoccoro, S.; Minghetti, G. *Inorg. Chem.* **2000**, *39* (21), 4749–4755.

(26) We thank Mr. Pietro Butti for determining the structure. Details have been submitted to the Cambridge Database.

(27) Roland, S.; Audouin, M.; Mangeney, P. *Organometallics* **2004**, *23* (12), 3075–3078.

(28) Sanford, M. S.; Love, J. A.; Grubbs, R. H. *J. Am. Chem. Soc.* **2001**, *123* (27), 6543–6554.

(29) Fantasia, S.; Petersen, J. L.; Jacobsen, H.; Cavallo, L.; Nolan, S. P. *Organometallics* **2007**, *26* (24), 5880–5889.

(30) Fantasia, S.; Jacobsen, H.; Cavallo, L.; Nolan, S. P. *Organometallics* **2007**, *26* (14), 3286–3288.

(31) Cárdenas, D. J.; Echevarren, A. M.; Ramírez de Arellano, M. C. *Organometallics* **1999**, *18*, 3337–3341.

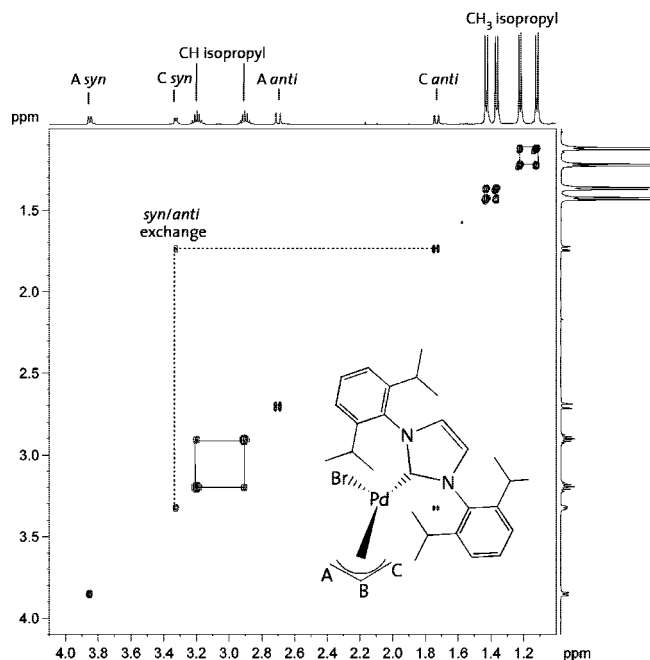
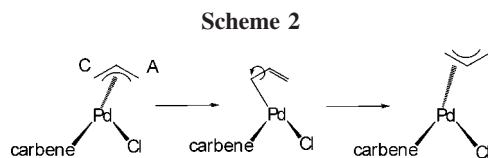


Figure 4. Section of the phase-sensitive ^1H NOESY spectrum for complex **1b**, showing the cross-peaks from the selective exchange processes involving the carbene isopropyl methyl groups and the allyl protons (CD_2Cl_2 , 500 MHz).

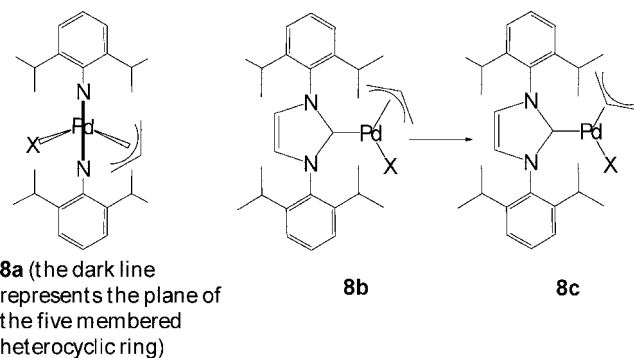


allyl cross-peaks reveals that there is *syn/anti* exchange only between the two protons on carbon C. This would be consistent with a selective η^3 - η^1 opening of the allyl under electronic control, rotation around the C-C bond, and then η^1 - η^3 isomerization to re-form the allyl ligand (see Scheme 2). This type of selectivity has been observed on a number of occasions.^{11,12} Given the structure of the carbene ligand, at the end of the isomerization process the allyl protons on carbon A find themselves in the same environment so that these do not show exchange cross-peaks. We find these dynamics for most of the complexes. However, for the SCN^- and CN^- complexes the phase-sensitive NOESY spectra do *not* show these exchange cross-peaks, and we thus estimate that the rates are now below ca. 0.1 s^{-1} .

Figure 4 also contains cross-peaks due to exchange between the two methine and four methyl *i*-Pr groups. Table 4 shows the rate constants that result from a series of magnetization transfer measurements,³² and several points are worth mentioning:

(a) The allyl isomerization and the isopropyl methyl exchange rates are not significantly different and (b) apart from the SCN^- and CN^- complexes, the iodide complex shows the slowest and the two O-donor ligands the fastest dynamics.

As indicated in **8a** (and supported by the X-ray data) the structure(s) of **1** will have the plane of the five-membered heterocyclic ring (dark line) almost perpendicular to the plane defined by the carbene-C, Pd, and X(donor) atoms. One can expect that the two aromatic rings will be, again, almost perpendicular to the plane of the five-membered heterocyclic ring, so that, although we only observe two methine CH-groups, in principle, there are four nonequivalent *i*-Pr environments. Although one observes an apparent AX_2 spectrum for the



aromatic ring protons (even in some cases down to 173 K in CD_2Cl_2 solution), the conventional ^{13}C spectrum in the aromatic region contains six signals, which, as reported previously,⁷ is consistent with rapid rotation around the Pd-C bond, but restricted rotation around the N-C(*i*-Pr) bonds.³³ Therefore, the same allyl isomerization that interconverts the *syn* and *anti* protons moves the η^3 - C_3H_5 from its position in **8b** to that for **8c** and thus explains the observed exchange dynamics for the *i*-Pr groups.

The CH_3CO_2^- and CF_3SO_3^- complexes **1h** and **1i** showed much broader ^1H lines at room temperature, suggesting faster exchange dynamics. For the CF_3SO_3^- complex, **1i**, the ^1H lines were fairly sharp at 273 K and the NMR and exchange data presented stem from measurements at this temperature. The ^{19}F spectrum shows a sharp resonance close to that of anionic triflate. Despite the fact that no signal that might have been assigned to coordinated water was detected, it was not immediately clear whether the complex should be formulated as $[\text{Pd}(\text{CF}_3\text{SO}_3)(\eta^3\text{-C}_3\text{H}_5)(\text{IPr})]$ or $[\text{Pd}(\text{H}_2\text{O})(\eta^3\text{-C}_3\text{H}_5)(\text{IPr})](\text{CF}_3\text{SO}_3)$. Addition of an excess of water to the solution resulted in essentially *no change* in any of the ^1H positions and (apart from the new water resonance) the appearance of a new line at $\delta = 2.11$, integrating for ca. 8H atoms. Therefore, we believe that we have the aquo cationic complex rather than the neutral triflate, in solution. The decision to consider the triflate anion as *not* coordinated was made using data from two further sources: (a) the PGSE diffusion measurements in CD_2Cl_2 at 298 K (see Table 5) are in very good agreement with anionic triflate and (b) the elemental analyses are more consistent with the aquo-complex. We note that both triflate and aquo-Pd allyl complexes have been suggested and isolated.⁷ The PGSE diffusion data for **1a**, **1c**, and **1i** afford hydrodynamic radii, r_{H} , that, after a literature correction,³⁴ are in excellent agreement with the $r_{\text{X-ray}}$ value obtained from the volume of the unit cell.

Pörschke¹⁶ has reported the synthesis of the dinuclear salt **9**.¹⁶ We do not favor this dinuclear structure for our triflate chemistry, as our diffusion data ($r_{\text{H}} = 5.6 \text{ \AA}$) suggest a mono—rather than a dinuclear product. The X-ray structure of **9** has been reported and affords an $r_{\text{X-ray}}$ of 7.7 \AA . The 2-D exchange spectrum for **1i** at 273 K is consistent with the same type of selective allyl isomerization mechanism observed for the chloro-complex.

(32) Sandstrom, J. *Dynamic NMR Spectroscopy*; Academic Press: London, 1982.

(33) We originally incorrectly assigned the restricted rotation to the Pd-C(carbene) bond. Restricted rotation of this type has been reported, but for *t*-butyl (and not *i*-Pr) substituents on the N-atom. (a) Burling, S.; Douglas, S.; Mahon, M. F.; Nama, D.; Pregosin, P. S.; Whittlesey, M. K. *Organometallics* **2006**, 25 (10), 2642–2648. (b) Burling, S.; Paine, B. M.; Nama, D.; Brown, V. S.; Mahon, M. F.; Prior, T. J.; Pregosin, P. S.; Whittlesey, M. K.; Williams, J. M. J. *J. Am. Chem. Soc.* **2007**, 129 (7), 1987–1995.

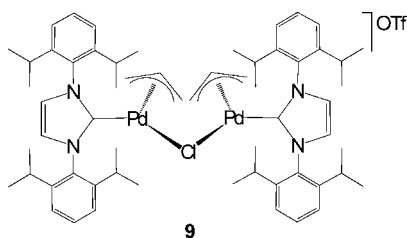
Table 4. Rate Constants for the Exchange Involving the Isopropyl and Allyl Groups (500 MHz in CD₂Cl₂ at 298 K unless otherwise stated)

	Cl		Br	I		N ₃	NCO	OAc (at 203 K)	OTf (at 273 K)
	CD ₂ Cl ₂	THF		CD ₂ Cl ₂	THF				
k_{carbene} (s ⁻¹)	1.4 ± 0.1	2.5 ± 0.1	1.0 ± 0.1	0.2 ± 0.1	0.1 ± 0.1	0.6 ± 0.1	1.0 ± 0.1	1.1 ± 0.1	6.0 ± 0.1
k_{allyl} (s ⁻¹)	1.3 ± 0.1	2.6 ± 0.1	0.8 ± 0.1	<0.1	<0.1	0.2 ± 0.1	0.8 ± 0.1	1.0 ± 0.1	6.2 ± 0.1

Table 5. Radii from Crystallographic Structures and PGSE Diffusion Measurements

	X-ray	PGSE diffusion	
	$r_{\text{X-ray}}$ (Å)	D (10 ⁻¹⁰ m ² /s)	r_{H} (Å) ³⁴
[PdCl(C ₃ H ₅)(IPr)], 1a	5.9 ⁸	10.57	5.6
[Pd(C ₃ H ₅)(IPr)], 1c	5.6	10.39	5.7
[Pd(H ₂ O)(C ₃ H ₅)(IPr)]OTf ^a , 1i dimer, 8	7.7 ¹⁶	10.57	5.6

^a Data for the cation. For the OTf⁻ anion: $D = 10.99$ and $r_{\text{H}} = 5.4$ Å. The fairly large value of the triflate hydrodynamic radius suggests that the anion may be hydrogen bonded to (and exchanging from) the bound water.



For the acetate complex, **1h**, the room-temperature ¹H spectrum reveals a broad two-proton allyl signal resulting from the coalescence of the *syn* and *anti* resonances of carbon C, in keeping with the isomerization mechanism described above. Support for complexed acetate comes from the observed NOE contacts between the methyl group of the acetate and one set of *i*-Pr methyl groups. The exchange cross-peaks from the phase-sensitive NOESY spectrum indicated exchange between coordinated acetate and a trace amount of free acetate; however, this exchange can be suppressed by cooling the sample to 203 K. At this temperature we *still observe* the selective allyl isomerization indicated above. The rate constant in Table 4 for the sample of **1h** as well as the ¹³C data given in Table 1 were obtained at 203 K.

The chemistry with 4-picoline was somewhat different. NMR analysis of the *isolated* reaction product which should lead to [Pd(η^3 -C₃H₅)(IPr)(4-MePy)], **1j**, in CD₂Cl₂ shows that some disproportionation had occurred and that both **1j** and the bis-4-picoline cation, [Pd(η^3 -C₃H₅)(4-MePy)₂]⁺ **10**, as the SbF₆ salt, were present in solution in about equal amounts. For **1j** we find no isomerization of the allyl ligand and assume that the observed ¹³C chemical shifts in **1j** are not strongly affected by the presence of **10**.

The question as to the source of the different rates of allyl isomerization remains. If a five-coordinate species were to be important, then a change to a potentially coordinating solvent might change the isomerization rates. To this end we have carried out a few measurements in THF-*d*₈ solution using the Cl⁻, I⁻, and CN⁻ complexes. For the chloride we find the dynamics to be faster by a factor of ca. 2, but for the iodide the rate seems unchanged. Further, we find no allyl exchange for the CN⁻ analogue in THF. For a solution of the Cl⁻ complex in THF, addition of an excess of water does *not* change either the allyl chemical shifts or the line widths within the experi-

mental error. Further, for the acetate sample, which contains a trace of free acetate, lowering the temperature blocks the intermolecular acetate exchange, but not the allyl isomerization. All of these observations are consistent with the mechanism of Scheme 2, rather than isomerization via a five-coordinate species.

If steric effects were important, then the larger X ligands should accelerate the allyl isomerization, and, if anything, the reverse is true, e.g., iodide slower than chloride; cyanide slower than either azide or isocyanate.

Conclusions

Assuming that we can consider the η^3 -C₃H₅ in **1** as a “small” to modest size ligand, then the observation that the carbene *trans* influence is substantial but not larger than a P-donor is interesting. In the absence of significant steric effects, the allyl ¹³C chemical shifts reflect the electronic bonding characteristics of the carbene, which for Pd(II) suggest a reasonable, but not very strong σ -donor.

Returning to the changes in the allyl dynamics, perhaps a modest electronic *cis* effect is responsible for this trend.²⁵ However, an alternative explanation involves using the observed low-frequency ¹³C chemical shifts as an indication of increased π -back bonding from the Pd to the allyl. The stronger X-donors favor more back bonding with the result that the allyl isomerization slows. Further, the Pd–C_A distances are consistent with this view; that is, the better donor iodide results in a shorter Pd–C_A bond. In any case all of these points invoke differences in electronic factors. The available evidence suggests a dissociative rather than an associative mechanism for the isomerization.

Experimental Part

General Procedures. All reactions and manipulations were performed under a N₂ atmosphere using standard Schlenk techniques. The palladium complex (IPr)Pd(C₃H₅)Cl (where IPr = (*N,N'*-bis(2,6-diisopropylphenyl)imidazol-2-ylidene)) was purchased from Strem Chemicals and used as received. Solvents were dried and distilled using standard procedures and stored under nitrogen. Infrared spectra were recorded using a Perkin-Elmer Spectrum BX FTIR spectrometer. Elemental analyses and mass spectroscopic studies were performed at the ETHZ.

NMR Measurements and Data Fitting. NMR spectra were recorded using Bruker Avance instruments operating at ¹H Larmor frequencies of 250, 300, 400, 500, and 700 MHz, and are referenced to TMS for ¹³C and ¹H and to liquid NH₃ for ¹⁵N. Chemical shifts are given in ppm; coupling constants (*J*) in hertz. The temperature was controlled by a Bruker BVT 3000 digital unit. Magnetization transfer experiments were performed by using the selective inversion-exchange/recovery monitoring scheme according to the literature.³⁵ For fitting the monitored data of the magnetization transfer experiments the CIFIT program package was used.³⁶ Phase-sensitive

(35) Led, J. J.; Gesmar, H. J. *Magn. Reson.* **1982**, 49 (3), 444–463.

(36) (a) The CIFIT program package was used for the simulations and data evaluation: Bain, A. D.; Cramer, J. A. *J. Magn. Reson. Ser. A* **1996**, 118, 21. (b) Muhandiram, D. R.; McClung, R. E. D. *J. Magn. Reson.* **1987**, 71, 187.

(34) Zuccaccia, D.; Macchioni, A. *Organometallics* **2005**, 24 (14), 3476–3486.

Table 6. Experimental X-ray Diffraction for [PdI(η^3 -C₃H₅)(IPr)] (1c)

formula	C ₃₀ H ₄₁ N ₂ Pd
mol wt	662.95
data coll. <i>T</i> , K	150 (2)
diffractometer	Bruker APEX II CCD
cryst syst	monoclinic
space group (no.)	<i>P</i> 2 ₁ / <i>n</i> (14)
<i>a</i> , Å	10.694(1)
<i>b</i> , Å	17.563(2)
<i>c</i> , Å	15.932(2)
β and θ , deg	96.757(1)
<i>V</i> , Å ³	2971.4(5)
<i>Z</i>	4
ρ (calcd), g cm ⁻³	1.482
μ , cm ⁻¹	16.83
radiation	Mo K α (graphite monochrom., $\lambda = 0.71073$ Å)
θ range, deg	2.18 < θ < 26.50
no. data collected	31 227
no. indep data	6140
no. obs reflns (<i>n_o</i>)	5287
[<i>F_o</i> ² > 2.0 σ (<i>F_o</i> ²)]	
no. of param.s refined (<i>n_v</i>)	322
<i>R</i> _{int} ^a	0.0271
<i>R</i> (obsd reflns) ^b	0.0267
<i>R</i> ² _w (obsd reflns) ^c	0.0606
GOF ^d	1.024

^a $R_{\text{int}} = \sum |F_o^2 - \langle F_o^2 \rangle| / \sum F_o^2$. ^b $R = \sum (|F_o - (1/k)F_c|) / \sum |F_o|$. ^c $R_w^2 = \{ \sum [w(F_o^2 - (1/k)F_c^2)^2] / \sum w[F_o^2]^2 \}^{1/2}$. ^d $\text{GOF} = [\sum_w (F_o^2 - (1/k)F_c^2)^2 / (n_o - n_v)]^{1/2}$.

NOESY were carried using the standard pulse sequence and a mixing time of 0.8 s.

Diffusion Measurements. The PGSE measurements³⁷ for the triflate complex **1i** were performed on a Bruker Avance spectrometer, 300 MHz, equipped with a microprocessor-controlled gradient unit and a multinuclear broadband probe with an actively shielded Z-gradient coil. The gradient shape was rectangular, and its length was 1.75 ms. Its strength was increased by steps of 3% during the course of the experiment. The time between midpoints of the gradients was 167.75 ms for all experiments. The experiments were carried out at a set temperature of 299 K within the NMR probe. Cation diffusion rates were measured using the ¹H signal from the imidazole CH group, and anion diffusion was obtained from the ¹⁹F signal of the triflate.

The PGSE diffusion measurements on model complexes **1a** and **1c** were performed on a Bruker Avance spectrometer, 700 MHz. The strength of the gradient was increased by steps of 4% during the experiment. The rest of the settings were the same as for complex **1i**. Complex diffusion rates were measured using the ¹H signal from the imidazole CH group.

The r_H values were calculated as suggested in the literature.³⁴

Crystallography. Air-stable, yellow crystals of **1c**, suitable for X-ray diffraction, were obtained by crystallization from dichloromethane/ether. A crystal was mounted on a Bruker APEX diffractometer, equipped with a CCD detector, and cooled, using a cold nitrogen stream, to 150(2) K for the data collection. The space group was determined from the systematic absences, while the cell constants were refined at the end of the data collection with the data reduction software SAINT.³⁸ The experimental conditions for the data collections and crystallographic and other relevant data are listed in Table 6 and in the Supporting Information.

The collected intensities were corrected for Lorentz and polarization factors³⁸ and empirically for absorption using the SADABS program.³⁹

The structure was solved by direct and Fourier methods and refined by full matrix least-squares,⁴⁰ minimizing the function $[\sum w(F_o^2 - (1/k)F_c^2)^2]$ and using anisotropic displacement parameters for all atoms, except the hydrogens.

The hydrogen atoms of the allyl moiety were located from the difference Fourier maps and their positions refined with isotropic temperature factors fixed at 1.3 $B(C_{\text{bonded}})$. The contribution of the remaining hydrogen atoms, in their calculated positions, was included in the refinement using a riding model ($B(H) = aB(C_{\text{bonded}})(\text{\AA}^2)$, where $a = 1.3$ for the hydrogen atoms of the methyl groups and $a = 1.2$ for the others). The scattering factors, corrected for the real and imaginary parts of the anomalous dispersion, were taken from the literature.⁴¹ All calculations were carried out by using the PC version of the programs: WINGX⁴² SHELX-97⁴⁰ and ORTEP.⁴³

Despite being unable to locate water in the proton spectra, the microanalytical data for many of the compounds suggest the presence of 1 to 2 equiv of water. The proton and carbon spectra do not indicate impurities or solvent.

Synthesis of [PdBr(C₃H₅)(IPr)] (1b). A solution of the palladium(II) complex (0.087 mmol, 1.0 equiv) and LiBr (0.262 mmol, 3.0 equiv) in acetone (5 mL) is stirred overnight at room temperature. The solvent is evaporated and the resulting solid is extracted with CH₂Cl₂ to remove the inorganic salts. To remove traces of LiCl and LiBr, the product is washed with water and dried under vacuum, to give a light yellow solid, yield 81%. ¹H and ¹³C and NMR data, see Table S1. Anal. Calcd for C₃₀H₄₁N₂PdBr·H₂O: C, 58.83; H, 6.84; N, 4.42. Found: C, 56.21, H, 6.43, N, 4.22. MALDI MS: 535 (M⁺ - Br), 495 (M⁺ - Br - C₃H₅), 389 (M⁺ - Br - C₃H₅ - Pd).

Synthesis of [PdI(C₃H₅)(IPr)] (1c). A solution of the palladium(II) complex (0.087 mmol, 1.0 equiv) and LiI (0.262 mmol, 3.0 equiv) in acetone (5 mL) is stirred overnight at room temperature. The solvent is evaporated and the resulting solid is extracted with CH₂Cl₂ to remove the inorganic salts. To remove traces of LiCl and LiI, the product is washed with water and dried under vacuum, to give a pale orange solid, yield 85%. ¹H and ¹³C and NMR data, see Table S1. Anal. Calcd for C₃₀H₄₁N₂PdI·H₂O: C, 52.91; H, 6.36; N, 4.11;. Found: C, 52.30; H, 6.10; N, 3.96. MALDI MS: 535 (M⁺ - I), 389 (M⁺ - I - C₃H₅ - Pd).

Synthesis of [PdN₃(C₃H₅)(IPr)] (1d). A solution of the palladium(II) complex (0.087 mmol, 1.0 equiv) and NaN₃ (0.873 mmol, 10.0 equiv) in acetone (5 mL) is stirred overnight at room temperature. During this time a white precipitate of NaCl is formed, which is removed by filtration. The solvent is evaporated and the resulting solid is extracted with CH₂Cl₂ to remove the inorganic salts. To remove traces of NaCl and NaN₃, the product is washed with water and dried under vacuum, to give a pale yellow solid, yield 90%. ¹H and ¹³C and NMR data, see Table S1. Anal. Calcd for C₃₀H₄₁N₅Pd·H₂O: C, 60.44; H, 7.27; N, 11.75. Found: C, 60.72; H, 7.07; N, 11.65.

Synthesis of [Pd(NCO)(C₃H₅)(IPr)] (1e). A solution of the palladium(II) complex (0.087 mmol, 1.0 equiv) and NaNCO (0.437 mmol, 5.0 equiv) in methanol (5 mL) is stirred overnight at room temperature. During this time a white precipitate of NaCl is formed, which is removed by filtration. The solvent is evaporated and the resulting solid is extracted with CH₂Cl₂ to remove the inorganic salts. The product is a yellowish solid, yield 82%. ¹H and ¹³C and

(39) Sheldrick, G. M. *SADABS*, Program for Adsorption Correction; University of Göttingen: Göttingen, Germany, 1996.

(40) Sheldrick, G. M. *SHELX-97*, Structure Solution and Refinement Package; University of Göttingen: Göttingen, Germany, 1997.

(41) *International Tables for X-ray Crystallography*; Kluwer Academic Publisher: Dordrecht, The Netherlands, 1992.

(42) Farrugia, L. J. *J. Appl. Crystallogr.* **1999**, *32*, 837.

(43) Farrugia, L. J. *J. Appl. Crystallogr.* **1997**, *30*, 565.

(37) (a) Pregosin, P. S.; Kumar, P. G. A.; Fernandez, I. *Chem. Rev.* **2005**, *105* (8), 2977–2998. (b) Pregosin, P. S. *Prog. Nucl. Magn. Reson. Spectrosc.* **2006**, *49*, 261–288.

(38) BrukerAXS, SAINT, Integration Software; Bruker Analytical X-ray Systems: Madison, WI, 1995.

NMR data, see Table S1. Anal. Calcd for $C_{31}H_{39}N_3OPd \cdot H_2O$: C, 62.67; H, 6.96; N, 7.07. Found: C, 63.14; H, 7.08; N, 6.91.

Synthesis of [Pd(SCN)(C₃H₅)(IPr)] (1f). A solution of the palladium(II) complex (0.087 mmol, 1.0 equiv) and NaSCN (0.437 mmol, 5.0 equiv) in acetone (5 mL) is stirred overnight at room temperature. During this time a white precipitate of NaCl is formed, which is removed by filtration. The solvent is evaporated and the resulting solid is extracted with CH₂Cl₂ to remove the inorganic salts. The product is a yellowish solid, yield 87%. ¹H and ¹³C and NMR data, see Table S1. Anal. Calcd for $C_{31}H_{41}N_3PdS \cdot H_2O$: C, 62.67; H, 6.95; N, 7.07. Found: C, 62.46; H, 6.99; N, 6.92. MALDI MS: 535 ($M^+ - SCN$), 389 ($M^+ - SCN - C_3H_5 - Pd$).

Synthesis of [Pd(CN)(C₃H₅)(IPr)] (1g). A solution of the palladium(II) complex (0.087 mmol, 1.0 equiv) and KCN (0.173 mmol, 2.0 equiv) in acetone (5 mL) is stirred overnight at room temperature. During this time a white precipitate of KCl is formed, which is removed by filtration. The solvent is evaporated and the resulting solid is extracted with CH₂Cl₂ to remove the inorganic salts. The product is a pale yellow solid, yield 79%. ¹H and ¹³C and NMR data, see Table S1. Anal. Calcd for $C_{31}H_{41}N_3Pd \cdot H_2O$: C, 64.18; H, 7.47; N, 7.27. Found: C, 64.86; H, 7.21; N, 7.54. MALDI MS: 535 ($M^+ - CN$), 389 ($M^+ - CN - C_3H_5 - Pd$).

Synthesis of [Pd(CH₃CO₂)(C₃H₅)(IPr)] (1h). A solution of the palladium(II) complex (0.087 mmol, 1.0 equiv) in CH₂Cl₂ is slowly poured into a Schlenk tube containing dry AgOAc (0.087 mmol, 1.0 equiv). A white precipitate forms immediately. The suspension is stirred for about 10 min, and then it is filtered over Celite. The solvent is removed and the resulting whitish solid is dried in vacuum, yield 85%. ¹H and ¹³C and NMR data, see Table S1. Anal. Calcd for $C_{32}H_{44}N_2O_2Pd \cdot 2H_2O$: C, 60.90; H, 7.66; N, 4.44. Found: C, 59.95; H, 8.01; N, 4.45.

Synthesis of [Pd(H₂O)(C₃H₅)(IPr)](CF₃SO₃) (1i). A solution of the palladium(II) complex (0.087 mmol, 1.0 equiv) in CH₂Cl₂ is slowly poured into a Schlenk tube containing dry AgOTf (0.096 mmol, 1.1 equiv). A white precipitate forms immediately. The suspension is stirred for 2 h at room temperature, and then it is filtered over Celite. The solvent is removed and the resulting whitish solid is dried in vacuum, yield 94%. ¹H and ¹³C and NMR data, see Table S1. Anal. Calcd for $C_{31}H_{41}F_3N_2O_3PdS \cdot H_2O$: C, 52.95; H, 6.16; N, 3.98. Found: C, 53.35; H, 6.00; N, 3.99. MALDI MS: 535 ($M^+ - OTf$), 389 ($M^+ - OTf - C_3H_5 - Pd$). The complex reacts with the matrix (3-HPA, 3-hydroxypicolinic acid) to give disproportionation products, 885 (IPr-Pd-IPr).

Synthesis of [(IPr)Pd(C₃H₅)(4-MePy)]SbF₆ (1j). A solution of the palladium(II) complex (0.087 mmol, 1.0 equiv) and 4-picoline (0.096 mmol, 1.1 equiv) in CH₂Cl₂ is slowly poured into a Schlenk tube containing AgSbF₆ (0.096 mmol, 1.1 equiv). A white precipitate forms immediately. The suspension is stirred for 2 h at room temperature, and then it is filtered over Celite. The solvent is removed and the resulting pale yellow solid is dried under vacuum, crude yield 95%. ¹³C NMR data for the allyl ligand, see Table 1.

Acknowledgment. P.S.P. thanks the Swiss National Science Foundation and the ETH Zurich for support, as well as the Johnson Matthey Company for the loan of palladium salts. A.A. thanks MURST for a grant (PRIN 2004).

Supporting Information Available: This material is available free of charge via the Internet at <http://pubs.acs.org>.

OM7010613